Neutral and Charged Excited States in Polar Organic Films: Origin of Unusual Electroluminescence in Tri-*p*-tolylamine-Based Hole Conductors

S. Mukhopadhyay,*,† B. J. Topham,‡ Z. G. Soos,‡ and S. Ramasesha†

Solid State and Structural Chemistry Unit, Indian Institute of Science, Bangalore 560012, India, and Department of Chemistry, Princeton University, Princeton, New Jersey 08544

Received: February 11, 2008; Revised Manuscript Received: April 28, 2008

The photoluminescence (PL) and electroluminescence (EL) of thin films of 1,1-bis[(di-4-tolylamino)phenyl]-cyclohexane (TAPC) are remarkably different. Similar PL and EL are instead observed in films of the closely related donors tri-*p*-tolylamine (TTA) and *N*,*N*′-diphenyl-*N*,*N*′-bis(3-methylphenyl)-(1,1′-biphenyl)-4,4′-diamine (TPD). Such films show a wide range of hole transport that depends on the morphology and on external parameters such as temperature and electric field. Restricted configuration-interaction calculations performed on TTA, TAPC, TPD, and radical ions of TTA indicate that the unusual EL of TAPC films is due to direct recombination from a low-lying charge-transfer (CT) state. The CT state is strongly stabilized by electrostatic interactions with the polar environment. Theory confirms that TAPC can be considered a dimer of TTA. The charge distributions of TTA^+ and TTA^- indicate charge localization in the anion that rationalizes low electron mobility as well as a strong charge−induced-dipole stabilization of the CT state.

I. Introduction

Recent advances in molecular electronics have exploited two remarkable and related properties of conjugated organic molecules. In the absence of intermolecular bonds, electronic and optical excitations in condensed phases are related to molecular excitations, as discussed in molecular exciton theories, and charges are largely localized on molecules, as expected in a low-dielectric medium. Frenkel excitons describe the solid-state photophysics of conjugated molecules, such as fluorescence from the lowest singlet excited state or phosphorescence from the lowest triplet state. Gas-phase energies change modestly by about 0.5 eV or less for such neutral excitations, consistent with small perturbations due to the environment. Electronics applications also call for charged excitations such as electrons, holes, and charge-transfer (CT) states that differ by an electron volt or more from gas-phase processes. Nevertheless, molecular wave functions are largely retained, and electrostatic interactions account for the energy of CT states or ion pairs in organic crystals of nonpolar molecules.

The present study was motivated by the striking electroluminescence (EL) of 1,1-bis[(di-4-tolylamino)phenyl]cyclohexane (TAPC) films reported by Kalinowski et al.,[1] who assigned the emission at 580 nm to an unspecified deep trap. We recently suggested[2] that the EL originates from direct recombination of an ion pair of tri-*p*-tolylamine (TTA) for two reasons, both qualitative. First, emission at similarly long wavelengths is well documented[3–5] in solutions containing TTA as the donor and is the exciplex route for chemiluminescence (CL) or electro-CL. Direct recombination is assumed from ion pairs in solution whose structure is not known. Second, Rommens et al.[6] reported dual EL with an emission peak between 575 and 595 nm in thin-film devices with a single or double layer of a substituted 1,3,5-triphenylbenzene, whose three TTA moieties are weakly coupled through the central phenyl ring. TAPC (Figure 1) is a TTA dimer with a σ-bonded bridge. Similar EL in different systems under different conditions points to an intrinsic phenomenon rather than a trap of some sort. However, the hypothesis of direct recombination of an ion pair clearly requires evidence for a CT state with unusually low energy. To that end, we have carried out extensive molecular calculations on TTA,

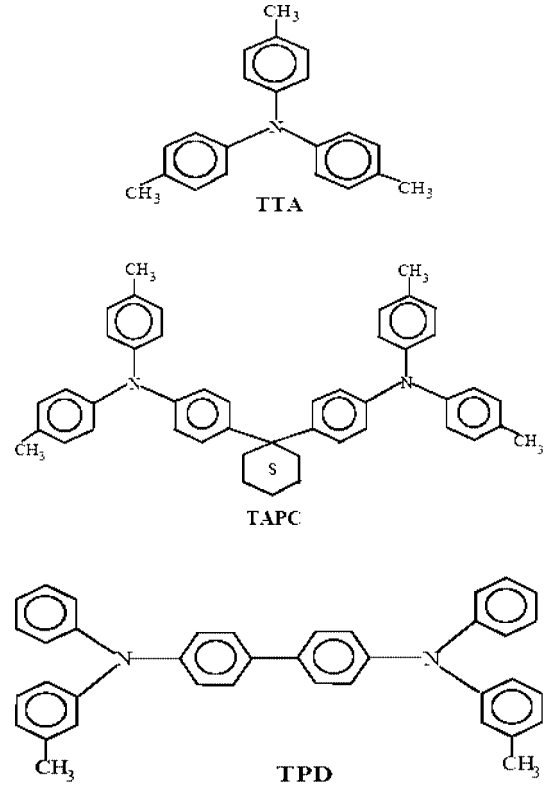

Figure 1. Molecular structures of tri-*p*-tolylamine (TTA), 1,1-bis[(di-4-tolylamino)phenyl]cyclohexane (TAPC), and *N*,*N*′-diphenyl-*N*,*N*′-bis(3-methylphenyl)-(1,1′-biphenyl)-4,4′-diamine (TPD).

* To whom correspondence should be addressed. E-mail: sukrit@sscu.iisc.ernet.in.
† Indian Institute of Science.
‡ Princeton University.

10.1021/jp8012078 CCC: $40.75
Published on Web 07/17/2008

TABLE 1: Optimized Geometries of TTA and Its Ions Obtained Using HF/4-31g and B3LYP/6-31g*[a]

system	method	C—N bond length(s) (Å)	∠CNC bond angle(s) (deg)	dihedral angles (deg)
TTA	HF/4-31g	1.42 (1.408−1.427)	120 (118−120)	48.60, 47.58, 47.72 (37.0−50.5)
	B3LYP/6-31g*	1.42	120	41.55, 41.48, 41.67
TTA^+	B3LYP/6-31g*	1.41	120	38.90, 38.96, 38.98
TTA^-	B3LYP/6-31g*	1.42, 1.40, 1.42	116.86, 121.55, 121.59	57.96, 54.15, 57.29

[a] Experimental values from ref 12 are in parentheses.

TABLE 2: Geometries of TAPC and TPD and Their Ions Obtained by B3LYP/6-31g*

system	unit	C—N bond length(s) (Å)	∠CNC bond angle(s) (deg)	dihedral angles (deg)
TAPC	TTA unit I	1.42	120	40.77, 41.12, 41.39
	TTA unit II	1.42	120	41.33, 41.87, 41.68
$TAPC^+$	TTA unit I	1.43, 1.40, 1.42	120.37, 118.85, 120.77	44.59, 42.28, 44.12
	TTA unit II	1.40, 1.43, 1.42	120.42, 120.69, 118.89	44.39, 44.24, 42.56
$TAPC^-$	TTA unit I	1.41, 1.43, 1.42	120.58, 118.14, 121.28	46.58, 42.97, 53.97
	TTA unit II	1.43, 1.42, 1.42	117.85, 121.57, 120.57	56.29, 48.20, 56.00
TPD	TTA unit I	1.42	120	42.66, 41.53, 41.76
	TTA unit II	1.42	120	40.67, 42.33, 42.66
TPD^+	TTA unit I	1.43, 1.43, 1.39	117.78, 121.13, 121.09	47.59, 49.04, 49.32
	TTA unit II	1.43, 1.43, 1.39	117.78, 121.13, 121.09	47.59, 49.04, 49.32
TPD^-	TTA unit I	1.41, 1.41, 1.44	121.80, 119.17, 119.09	34.94, 31.54, 31.81
	TTA unit II	1.41, 1.41, 1.44	121.80, 119.17, 119.09	34.94, 31.54 31.81

TAPC, and *N*,*N*′-diphenyl-*N*,*N*′-bis(3-methylphenyl)-(1,1′-biphenyl)-4,4′-diamine (TPD) to obtain gas-phase excitation energies and molecular properties. The molecular properties were then used to model electrostatic interactions in amorphous polar films. The overall stabilization of a TTA^+TTA^- ion pair supports the hypothesis that EL is due to direct recombination.

As emphasized by Kalinowski et al.,[1] the narrow 580-nm EL of TAPC films is quite distinct from the 380- and 450-nm peaks observed in the photoluminescence (PL) of the same films. PL involves singlet excited states of molecules or small aggregates and has been so assigned in solution CL studies and in the solid state. Indeed, closely similar PL and EL in organic devices based on small molecules and conjugated polymers is decisive evidence that injected electrons and holes recombine to form a singlet exciton that subsequently emits a photon. Direct recombination of an ion pair requires a low-energy CT state, well below that of a singlet exciton. Such CT states are very rare in the organic condensed phase, but less so in polar solvents[3–5] whose dipoles can reorient around cations and anions. These observations point to electrostatic interactions in a polar medium for understanding long-wavelength EL.

In the present work, we analyze large energy shifts of ion pairs in amorphous polar films. The polar donors (D) in Figure 1 are aromatic amines that have been extensively studied as hole conductors in xerography.[7–9] Quantum chemical methods are widely applied to molecular excitations in the gas phase. TTA and related Ds are polar and have low-energy hindered rotations about single bonds. Quantum chemical methods also yield ionization potentials (IPs) and, less reliably, electron affinities (EAs) that are needed for charged excitations. In molecular materials, holes and electrons are associated with the ground states of cation and anion radicals, respectively,[10] whereas CT states in crystals are modeled as pairs of ions at fixed separation in the lattice.[11] Randomly oriented dipoles in amorphous films of TTA, TAPC, and TPD stabilize both charges and ion pairs as discussed below.

This article is organized as follows: Section II presents density functional (DFT) calculations of ground-state properties of the donors in Figure 1 and their ions. We obtain charge distributions and reorganization energies associated with charge redistribution and consider the possibility of charge localization. Section III presents results from the Pariser−Parr−Pople (PPP) model for singlet and triplet excited states that are compared to solution data. TAPC has decoupled π systems, whereas TPD does not. The intramolecular CT excitation of TAPC was found self-consistently and is strongly stabilized by charge−induced-dipole interactions. We turn in section IV to interactions with the polar environment in amorphous films that we model as a lattice whose density, dipoles, and polarizabilities are taken from experiment. The electronic stabilization of an ion pair is much larger in films with fixed dipoles than in solutions with reorientable dipoles. The final section summarizes the special properties of TAPC leading to its red-shifted EL.

II. Ground-State Properties

II.1. Geometries of Molecules and Ions. This section focuses on ground electronic states and molecular geometry. We employed two different techniques, namely, a Hartree−Fock (HF) calculation with a 4-31g basis and a density functional (DFT) calculation with the B3LYP/6-31g* basis. However, in both calculations, we retained the planarity of the phenyl rings. We optimized the geometry by varying the C—N bond lengths, CNC bond angles, and the dihedral angles between a phenyl ring and the plane formed by N and its C-atom neighbors. The TTA structure is presented in Table 1 and is almost the same for the two schemes.

There is a difference of 6° in the dihedral angles for the two calculations. B3LYP/6-31g* is known to give better geometries for such molecules because it includes the 3d orbitals of N and C atoms, which affects the C—N bonds significantly. Experimentally, the crystal structure[12] of TTA has been solved, and the molecular geometry parameters obtained are also included in Table 1. The optimized geometries for TAPC and TPD were obtained using the B3LYP/6-31g* method, and the structural parameters obtained are reported in Table 2. The similarity of the structural parameters of TAPC and TTA leads us to conclude that TAPC can be viewed as a dimer of TTA. Very similar absorption and PL spectra of TTA and TAPC observed in solution[1] strengthen our argument. However, TPD cannot be considered as a dimer of TTA because the conjugation is not completely broken between the two TTA units constituting TPD.

II.2. Charge Gap and Reorganization Energy. An important property of molecular conductors is the transport gap, E_t,

TABLE 3: Reorganization Energies (eV) for Electron and Hole Transfer in TTA, TAPC, and TPD[a]

	electron transport		hole transport	
system	λ_i^-	λ_n^+	λ_i^-	λ_n^+
TTA	0.11	0.16	0.06	0.06
TAPC	0.11	0.13	0.05	0.05
TPD	0.27	0.27	0.13	0.15

[a] λ's are defined in eq 2.

TABLE 4: Dipole Moments in the Ground States of TTA, Its Ions, TAPC, and TPD[a]

system	dipole moment (D)
TTA	0.62 (0.87)
TTA^+	0.90
TTA^-	9.76
TAPC	1.09 (1.41)
TPD	0.21 (1.52)

[a] Experimental values from ref 15 in parentheses.

which contains both molecular and solid-state contributions.[13] The molecular part of E_t is the charge gap in the gas phase

$$E_{cg} = \mathrm{IP} - \mathrm{EA} \tag{1}$$

where IP is the ionization potential and EA is the electron affinity. Because these quantities involve the ground states of molecules and ions, we calculate E_{cg} using B3LYP/6-31g* for TTA and distinguish between the vertical and adiabatic charge gaps. The vertical gap, $E_{cg}(v) = 7.43$ eV, is based on the optimized TTA geometry. The adiabatic gap, $E_{cg}(ad) = 7.04$ eV, also has the optimized geometry for the ions. The difference between the vertical and adiabatic gaps is the intramolecular part of the reorganization energy, λ, in Marcus theory.

Accordingly, we use λ_i for the reorganization energy of ions and λ_n for the reorganization energy of the molecule in the geometry of the ions. We define

$$\begin{aligned} \lambda_i^{\pm} &= E_n(\mathrm{TTA}^{\pm}) - E(\mathrm{TTA}^{\pm}) \\ \lambda_n^{\pm} &= E_{\pm}(\mathrm{TTA}) - E(\mathrm{TTA}) \end{aligned} \tag{2}$$

where E(TTA) and E(TTA $^{\pm}$) indicate the relaxed ground-state energy of the indicated species, whereas E_n and $E_{\pm}$ indicate the energies at the geometries at which the ions and molecules, respectively, were calculated. Table 3 lists reorganization energies for TTA, TAPC, and TPD computed at the B3LYP/6-31g* level. This ensures that the C—N bonds are properly optimized.[14] The (gas-phase) hole transfer, $D + D^+ \rightarrow D^+ + D$, has $\lambda_h = \lambda_i^+ + \lambda_n^+$, and similarly for electron transfer between D and D^-. The sum of the reorganization energies of any row of the table is the gas-phase reorganization energy of E_{cg} for the species.

The values in Table 3 are in good agreement with previously calculated reorganization energies for triphenylamine.[14] Similar λ_n^+ and λ_i^+ values indicate that the molecule and cation have parabolic potential energy surfaces with similar curvatures at equilibrium. This is indeed quite common in acene-type molecules.[11] As expected, the reorganization energy of TAPC is found to be very similar to that of TTA, whereas that of TPD is slightly higher.

The dipole moments in Table 4 were calculated at the HF level. The TTA, TAPC, and TPD dipole moments are in fair agreement with measurements in solution. As previously noted,[15] however, the dipoles of triarylamines such as TTA are easily perturbed in condensed phases and reflect deviations from a planar C_3 structure. The crystal structures of TTA and of three molecules with the methyl group at the meta position in one, two, or all three phenyls illustrate such variations.[16] The dipole moments of TTA ions in Table 4 were calculated relative to the center of charge.

The large dipole of TTA^- can be understood in terms of the ground-state π-electron charge distributions shown in Figure 2 and calculated using the PPP model (see section III.1). Although slightly different, the dihedral angles of the phenyl rings in Table 1 are nearly the same in TTA and the cation. Hence, the charge distribution is almost symmetric, and the dipole is small. The anion, by contrast, shows substantial (0.75) charge localization on the phenyl with the smallest dihedral angle. The calculated dipole represents a 2-Å displacement of an electron. Because the dipole can be rotated among three minima by interchanging dihedral angles, the anion's polarizability is expected to be exceptionally large.

III. Excited States of TTA, TAPC, and TPD and Their Ions

III.1. PPP Hamiltonian. Molecules such as TTA, TAPC, and TPD are large conjugated systems in which $\sigma-\pi$ separability[17] is expected to be an accurate approximation. The low-lying excitations of such systems are predominantly due to π electrons. The orbitals involved in the conjugation are the p_z orbitals of the sp^2 carbons and the orbital containing the lone pair of the central nitrogen atom. To account for the long-range Coulomb interactions, we employed the PPP model[17] to study these systems. The central N atom is sp^2 hybridized mainly because of steric effects. In the optimized structures in Tables 1 and 2, the N atom and the three C atoms bonded to it lie in a plane. The PPP Hamiltonian in the basis of the atomic orbitals (AOs) involved in conjugation is given by

$$\hat{H}_{PPP}^{AO} = \sum_{\langle ij\rangle,\sigma} \beta_{ij}(\hat{a}_{i,\sigma}^{+}\hat{a}_{j,\sigma} + hc) + \sum_{i,\sigma} \alpha_i \hat{n}_{i,\sigma} + \sum_i \frac{U_i}{2}\hat{n}_i(\hat{n}_i - 1) + \sum_{i>j} V_{ij}(\hat{n}_i - z_i)(\hat{n}_j - z_j) \tag{3}$$

Here, $\hat{a}_{i,\sigma}^{+}$ ($a_{i,\sigma}$) creates (annihilates) an electron with spin σ in the atomic orbital at site i, and $\hat{n}_{i,\sigma}$ is the corresponding number operator. α_i represents the energy of site (orbital) I, β_{ij} gives the transfer or resonance integral between the chemically bonded sites i and j, and the summation in the first term extends over bonded pairs ij. U_i is the Hubbard repulsion parameter and corresponds to the electron repulsion integral between two electrons in the same orbital i, z_i is the occupation number of orbital i when that orbital is electrically neutral, and V_{ij} is the intersite electron repulsion integral between sites i and j. We parametrized V_{ij} using the Ohno scheme[18] as follows

$$V_{ij} = 14.397\left[\left(\frac{28.794}{U_i + U_j}\right)^2 + r_{ij}^{\,2}\right]^{-1/2} \tag{4}$$

The PPP Hamiltonian spans a large Hilbert space whose dimensionality increases exponentially with the system size.

The largest system for which the low-lying states of the PPP Hamiltonian have been obtained exactly has 16 nearly half-filled orbitals, in a low-symmetry environment. Beyond this size, exact solution is not computationally feasible at present. The TTA molecule has 19 orbitals (18 carbon p_z orbitals and 1 nitrogen p_z orbital) and 20 electrons in conjugation, whereas its "dimer" TAPC has 38 sites and 40 electrons. Although the conjugation between two TTA units is broken in TAPC, Coulomb interactions prevent the factoring of TAPC into two

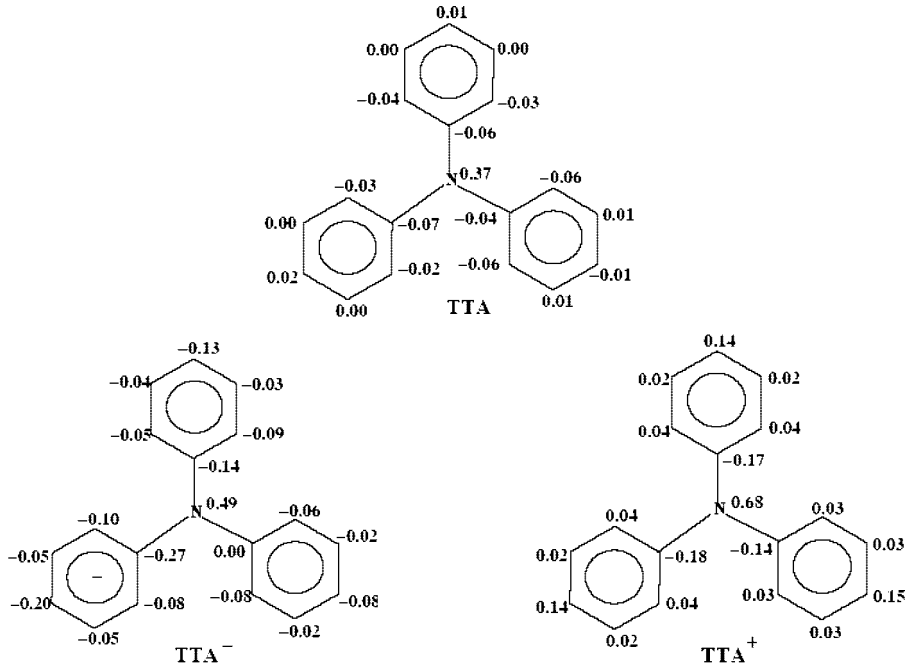

Figure 2. Site charge densities of TTA, TTA^-, and TTA^+. The optimized structure of the neutral molecule was used for the radical ions.

independent TTA units. The standard method for tackling large systems is to resort to approximations that are best implemented in the molecular orbital (MO) basis. The PPP Hamiltonian in the AO basis (eq 3) can be transformed into a MO basis according to the relation

$$\hat{b}^{+}_{i,\sigma} = \sum_{\mu} c_{\mu,i}\hat{a}^{+}_{\mu\sigma} \tag{5}$$

where $c_{\mu,i}$ is the coefficient of the μth AO in the ith MO, with energy ϵ_i. The molecular orbitals can be obtained from PPP Hamiltonian using the usual mean-field approximation. The PPP Hamiltonian in the MO basis is given by

$$\hat{H}^{\mathrm{MO}}_{\mathrm{PPP}} = \sum_{i,\sigma} \varepsilon_i \hat{b}^{+}_{i,\sigma}\hat{b}_{i,\sigma} + \frac{1}{2}\sum_{ijkl} W_{ijkl}(\hat{B}_{ij}\hat{B}_{kl} - \delta_{jk}\hat{B}_{il}) + \frac{1}{2}\sum_{ij} X_{ij}\hat{B}_{ij} + \frac{1}{2}Z \tag{6}$$

where W_{ijkl} gives the two-electron integrals in the MO basis related to the PPP interaction parameters, by

$$W_{ijkl} = \sum_{\mu} c_{\mu i}c_{\mu j}c_{\mu k}c_{\mu l}U_{\mu} + \sum_{\mu\nu} c_{\mu i}c_{\mu j}c_{\nu k}c_{\nu l}V_{\mu\nu} \tag{7}$$

The parameters X_{ij} and Z, defined in eq 8, arise as a result of the local chemical potentials, z_μ, in the PPP Hamiltonian

$$X_{ij} = \sum_{\mu\nu} (c_{\mu i}c_{\mu j}z_{\nu} + c_{\nu k}c_{\nu l}z_{\mu})V_{\mu\nu}$$
$$Z = \sum_{\mu\nu} V_{\mu\nu}z_{\mu}z_{\nu} \tag{8}$$

The parameters W_{ijkl}, X_{ij}, and Z were calculated using eqs 7 and 8. Because the Hamiltonian is spin-independent, we used the VB basis, which consists of eigenfunctions of S^2 and S^z, constructed from the MOs employed as one-particle basis functions. Because $H^{\mathrm{PPP}}_{\mathrm{MO}}$ contains terms such as W_{ijkl}, which scales as N^4, where N is the number of MOs, within a restricted CI scheme, excitations beyond two particle−hole excitations have to be neglected. One of the well-known problems associated with restricting the configuration space is size inconsistency,[19] which can be avoided if only single particle−hole excitation is considered in the many-body basis. This is the single configuration interaction (SCI) approximation, which is known to represent correctly the excitation energies.

The atomic parameters α_i, β_{ij}, and U_i in the PPP Hamiltonian are dependent on the hybridization and local environment of the particular atom.[20] The most widely used values for benzylic π bonds and their p_z carbon orbitals are −2.4 eV for β_{ij} and 11.26 eV for U_i. Because the zero of the potential can be fixed at any arbitrary value α_i, for homonuclear molecules in which all atoms are in identical chemical environments, all α_i values are usually taken to be zero to fix the energy scale. In TTA, there is a nitrogen atom that is sp^2 hybridized and connected to the benzylic carbon atoms. At the para position (with respect to the nitrogen atom), there are methyl groups attached to the benzylic carbon atom. Carbon atoms attached to nitrogen are slightly electron-deficient (slightly more electronegative than a benzylic carbon atom) because of the "−I" (electron-withdrawing) effect of the nitrogen atom. Similarly, the benzylic carbons attached to methyl groups are electron-rich (slightly less electronegative than a benzylic carbon atom) because of the "+I" (electron-donating) effect of the methyl group. To mimic these effects, α_is for these two types of carbon atoms are taken to be different from those for other benzylic carbon atoms. The more electronegative carbon atom is chosen to have lower α_i value (with respect to a benzylic carbon atom) to facilitate electron flow into the atom, whereas the one that is less electronegative is assigned a higher α_i value (with respect to a benzylic carbon atom). The nitrogen atom, with a higher atomic number, has more compact and stable p_z orbitals than the carbon atom. Therefore, α_N is taken to be lower than α_C and U_N slightly higher than U_C. The parameters employed in the PPP model are listed in Table 5.

To incorporate the effects of geometry on the transfer integrals, we used the Slater−Koster[21] method to modify β_{ij} values. The β_{ij} values depend on the overlap of the orbitals at atoms i and j and, thus, in turn, depend on their relative geometry. Because we are using $\sigma-\pi$ separability, we are concerned only with the relative orientation of the p_z orbitals

TABLE 5: PPP Parameters for TTA, TAPC, and TPD in the Ground-State Geometry

system	unit	α_N (eV)	U_N (eV)	α_C (eV)	β_{C-N} (eV)
TTA	–	−12.00	12.50	−0.25,[a] 0.25[b]	−2.56, −2.95, −2.41
TAPC	TTA unit I	−12.00	12.50	−0.25,[a] 0.25[b]	−2.73, −2.32, −2.83
	TTA unit II	−12.00	12.50	−0.25,[a] 0.25[b]	−2.77, −2.88, −2.33
TPD	TTA unit I	−12.00	12.50	−0.25,[a] 0.25[b]	−2.83, −2.64, −2.34
	TTA unit II	−12.00	12.50	−0.25[a], 0.25[b]	−2.34, −2.64, −2.85

[a] C bonded to N; [b] C bonded to methyl.

TABLE 6: Vertical Singlet and Triplet Excitation Energies (eV) of TTA, TAPC, and TPD and Oscillator Strengths of Singlets[a]

system	singlet (eV)	oscillator strength (10^{-1})	triplet (eV)
TTA	4.02(4.13)[4.16]	4.19(0.75)[2.32]	2.84(∼3.0)
	4.07	3.58	
	4.46	0.40	
	4.51	0.26	
	4.53	0.22	
TAPC	3.94(4.13)[4.19]	7.77(0.68)[4.27]	2.88(2.93)
	4.06	1.73	
	4.07	1.96	
	4.13	4.68	
	4.49	0.29	
TPD	3.55(3.35)[3.76]	11.48(0.49)[9.14]	2.69(2.34)
	4.02	1.59	
	4.03(3.97)[4.22]	6.63(0.44)[4.52]	
	4.17	0.24	

[a] Experimental energies and intensities in parentheses; ZINDO results in brackets.

located on each of the atoms. Carbon atoms in a ring are in the same plane, whereas atoms in different rings are in different planes mainly to reduce the steric effects of the bulky tolyl groups. Therefore, the p_z orbital on the nitrogen atom makes different angles with those of the carbon atoms bonded to it. Fixing the coordinate axis at the nitrogen atom and its p_z orbital along the z direction, we calculated the direction cosines with the carbon atoms, which, when multiplied appropriately by the in-plane value, gives the geometry-optimized β_{ij} values. The overlap integral between two p_z orbitals depends on the nature of the overlap (the overlap integral is different for σ and π bonds). Considering $\beta_{pp\sigma} = -3.0$ eV and $\beta_{pp\pi} = -2.32$ eV, the β_{C-N} values for three different C—N bonds in TTA and its derivatives are also included in Table 5.

The transfer integral for the bond connecting the two TTA units in TPD is taken to be 2.0 eV. The difference in β_{C-N} values between TTA and its derivatives (TAPC, TPD) is because the TTA units have different orientations of phenyl rings attached to two nitrogen atoms. The α_C values for the rest of the carbon atoms were taken to be zero.

III.2. Excitation Energies of Molecules and Ions. We performed PPP-SCI calculations on TTA, TAPC, TPD, and TTA ions in their ground-state geometries (section II). In addition to vertical excitation energies, we computed transition dipoles and oscillator strengths of low-lying singlets and doublets. Tables 6 and 7 summarize results for the most important states related to the photophysics. Experimental values are from ref 1 for TTA and TAPC singlets; ref 22 for TPD singlets; and refs 23 and 24 for the TTA, TAPC, and TPD triplets. We also performed semiempirical ZINDO[25] calculations that are much faster and fairly reliable. As expected, the lowest excitation of TTA involves intramolecular CT from N to phenyls. The five transitions between 4.02 and 4.53 eV in Table 6 are due to the different orientations of the rings that generate the PPP parameters in Table 5.

TABLE 7: Vertical Excitation Energies and Oscillator Strengths of TTA^+ and TTA^- Radical Ions

system	gap (eV)	oscillator strength (10^{-1})
TTA^+	2.51	0.05
	2.67	1.28
	2.67	0.04
	2.74	0.05
	2.80	1.11
TTA^-	0.35	0.42
	0.51	0.02
	0.64	0.01
	0.98	0.002
	1.77	1.79

The lowest ZINDO excitation is at 4.16 eV, and its oscillator strength of 2.32 is comparable to the PPP-SCI result for the 4.07 eV transition. The absorption maximum of TTA in solution is 4.1 eV, fully consistent with the calculated vertical excitation. Also listed in Table 6 are the vertical PPP-SCI excitations to the lowest triplet states of TTA, TAPC, and TPD. The experimental values are phosphorescence maxima that represent vertical transitions from the triplet geometry. The relaxed triplet of TTA at the B3LYP/6-31g* level is at 3.13 eV.

TTA has a stable cation radical whose solution spectrum has maxima at 1.82 and 2.14 eV.[26] The calculated transitions in Table 7 range from 2.51 to 2.80 eV, again due to the different orientations of the phenyl rings. The cation's lowest two excited states are calculated to have large dipoles of 17.35 and 18.04 D whose interaction with a polar solvent would lower the excitation energy. Although the TTA anion is not expected to be stable in solution, its PPP-SCI spectrum can readily be calculated. Electron localization on different rings and PPP parameters lead to four excited states below 1.0 eV with small transition dipoles (Table 7).

The radical ions of TTA and TAPC have similar excitation energies. This is due to the localization of the extra hole or electron on one of the TTA units in TAPC. In a noninteracting picture, in the case of the anion, the extra electron is in the doubly degenerate lowest unoccupied molecular orbital (LUMO) of one of the benzene rings, leading to strict six-fold degeneracy. However, electron−electron interactions in the PPP model marginally lift the degeneracy of these six low-lying states. Similar arguments can be posed for the near degeneracy of the first excited state of TTA^+ where the hole hops from the nitrogen atom to the phenyl rings. The charge density plots of the TTA^+, TTA^- and TTA are shown in Figure 2.

Because TAPC behaves as two TTA units, we were interested in its intramolecular CT excitation leading to a TTA^+TTA^- ion pairs. The vertical PPP-SCI excitation is 5.60 eV, some 1.5 eV above the singlet excitation of TAPC, but this does not include the mutual polarization of ions. Such a correction, primarily of polarization of the anion by the cation, is the Rittner model for alkali halides.[27] In addition, the structural relaxation of molecular ions has to be considered. We computed the π-electronic polarization energy of relaxed TTA ions arranged in the calculated geometry of TAPC. As discussed previously,[28] the Coulomb potential of π-electron charges, ρ_k, at carbon atom k are site energies $\epsilon_p = \Sigma_k \rho_k / R_{kp}$ at carbon atom p of the anion and vice versa. Self-consistent charges can be found for separate π systems with electrostatic interactions. The first step is to repeat the PPP-SCI calculation of each ion in the potential due to an isolated ion; the new charges produce an updated potential, and the process is repeated until ρ_k and ρ_p have converged. The self-consistent π charges of the relaxed ions stabilize the CT state by 0.93 eV relative to 5.60 eV. This large and purely

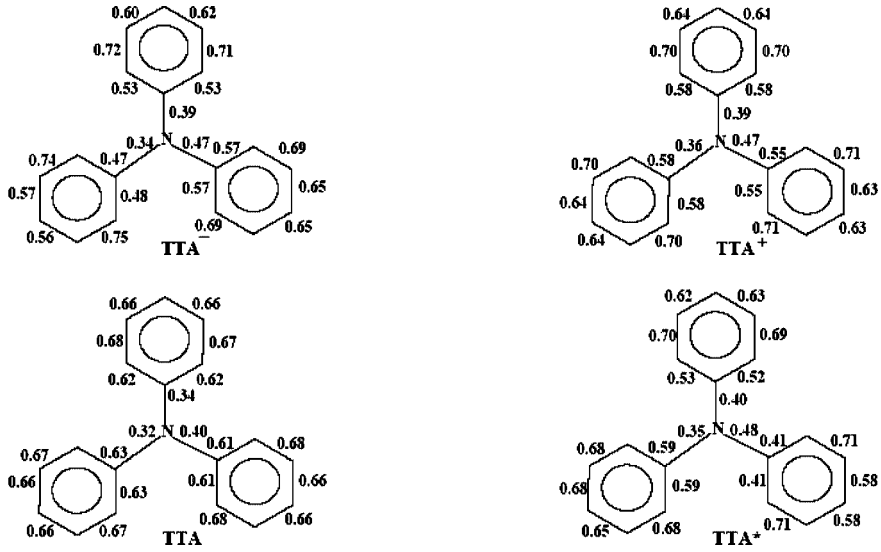

Figure 3. Bond orders in the ground states of TTA^-, TTA^+, and TTA and the first excited singlet state of TTA (TTA*).

electronic energy reflects both charge localization on TTA^- and π-electron polarizability. CT gives a large dipole of 36 D to TTA^+TTA^- that interacts with a polar medium.

III.3. Relaxation Energies of Excited States. Figure 3 shows PPP results for π-electron bond orders in the ground states of TTA, TTA^+, and TTA^- and the lowest singlet excited state, TTA*. Whereas the ground-state energies in the relaxed geometries can be computed in the B3LYP/6-31g* approximation, the relaxation energies of excited states cannot be obtained with this technique. However, we can couple the PPP Hamiltonian to the phonons to estimate the excited-state relaxation energy relative to the ground state. The electron−phonon coupling constant ($\lambda = 0.1$) was considered to be same for all bonds. Bond distortions were introduced so that the total of all bond orders remained constant; otherwise, the π-electron calculation would collapse the molecule to a point. In reality, the σ framework and the internuclear potentials prevent such a collapse.[29] The Hamiltonian including electron−phonon interaction is given by

$$H_{\mathrm{PPPP}} = H_{\mathrm{PPP}} + \frac{1}{\pi\lambda}\sum_i \delta_i^2 \tag{9}$$

Introducing the constraint, $L = \xi\sum_i\delta_i$ (where L is a constant and ξ is the Lagrange multiplier) and minimizing H_{PPPP}, we obtain $\xi = \bar{p}$, the average bond order in the chosen state, where the equilibrium distortion, δ_i, of a bond in the chosen excited state is given by

$$\delta_i = \pi\lambda(p_i - \bar{p}) \tag{10}$$

with p_i and $\bar{p}$ being the bond orders of the ith bond in the particular state and in the ground state, respectively. Therefore, the excited states are calculated both in the ground-state geometry and in relaxed geometries by a self-consistent calculation where the bond lengths and therefore the transfer integrals are changed iteratively according to the equations[30,31]

$$\begin{aligned} L_\rho &= L_1 - 0.78(\rho^{0.33} - 1) \\ t_{\mathrm{C-C}} &= -2.40 + 4.59(r_{\mathrm{C-C}} - 1.397) \\ t_{\mathrm{C-N}} &= -2.32 + 4.59\times(r_{\mathrm{C-N}} - 1.42) \end{aligned} \tag{11}$$

where L_ρ is the bond length corresponding to bond order ρ and L_1 is the bond length of a single bond. (For C—C bonds, L_1 is 1.54 Å, and for C—N bonds, L_1 is 1.47 Å.)

The bond orders of the ground states of TTA and TTA^+ are symmetric except at the bonds connecting N to the phenyl rings. One of the C—N bonds has a much lower bond order than the other two in the ground state. This can be rationalized considering the geometry of TTA where the benzene rings move out of plane. For TTA^- in the ground state, the bond orders of the C—C bonds in one of the rings is lower than those in the other two, clearly indicating that the extra electron is localized on the ring. This conclusion was also reached from the charge-density plots of TTA^-.

The calculated relaxation energy of the singlet excited state of TTA is 0.26 eV. The PL emission maximum for TTA or TAPC in solution[1] is at 370 nm (3.35 eV). The observed Stokes shift between the absorption and emission maxima is 0.78 eV. The low-energy TTA singlets in Table 6 indicate both high polarizability and the possibility of charge localization in polar solvents that would increase the Stokes shift, but we have not pursued such contributions.

IV. Electrostatic Energy Shifts in Amorphous Polar Films

The ground states in section II and the excited states in section III are generally in agreement with solution spectra. Although agreement to 0.5 eV or better is now expected for molecular excitations, we felt such confirmation to be necessary for TTA and TAPC in order to address the unusual 580 nm (2.13 eV) electroluminescence (EL) of TAPC films. In solutions containing TTA as the donor, exciplex emission at comparable energy is interpreted as direct recombination of ion pairs.[3,4] We suggested[2] that EL at 580 nm originates from TTA^+TTA^- ion pairs, but could not distinguish between unimolecular and bimolecular TAPC processes. In either case, vertical emission is from relaxed ions, whereas the corresponding vertical excitation (5.60 eV) is from the ground state of the neutral molecule. The gas-phase charge-gap difference for TTA is calculated in section II to be $E_{\mathrm{cg}}(\mathrm{v}) - E_{\mathrm{cg}}(\mathrm{ad}) = 0.39$ eV. Stabilization due to electronic polarization of the ions is 0.93 eV. The EL maximum of the intramolecular CT is estimated to be 4.28 eV before taking into account the polar medium.

Although molecular identity is largely retained in organic solids, electrostatic interactions can lead to large energy shifts.

The transport gap for injecting an electron and hole at infinite separation is related to the gas-phase charge gap by solid-state shifts[13]

$$E_t = \mathrm{IP} - \mathrm{EA} - P_+ - P_- + E_{cd} + ... \qquad (12)$$

Here, P_+ and P_- are the electronic polarization energies of the hole, taken as a cation, and the electron, taken as an anion, respectively. E_{cd} is the charge−dipole interaction in a polar medium. Additional (multipolar) electrostatic interactions can be considered but are expected to be small. It is implicitly assumed that electron transfer does not alter van der Waals or nonbonded interactions. The same approximations are used to estimate CT states or ion pairs at separation R in organic molecular crystals[11,32]

$$E_{CT}(R) = E_t + V(R) \qquad (13)$$

At large separation, the interaction V(R) is attractive and given by $-e^2/\kappa R$ in a medium with dielectric constant κ. The high-frequency or electronic dielectric constant $\kappa_\infty \approx 3$ enters in solids with fixed dipoles. $V(R)$ deviates from $1/R$ at small R for anisotropic organic molecules. When the crystal structure is known, electronic polarization and $E_{CT}(R)$ can be calculated self-consistently.[32]

We previously estimated $P_\pm$ and E_{cd} using a lattice model for TTA films.[2] TTA dipoles of ∼1 D account well for the energetic disorder $\sigma \approx 0.1$ eV deduced from modeling hole mobilities.[33] In the present work, we computed molecular excitation and relaxation energies, and we now use a lattice model for the stabilization energy of an ion pair. The stabilization is that of a dipole, because the direct interaction between TTA^+ and TTA^- has already been treated explicitly. We introduce a face-centered-cubic lattice with nearest-neighbor separation $d = 8$ Å. The volume per site is 360 Å^3, some 10% less than the molecular volume in TTA crystals.[12] At each lattice point, we place a randomly oriented, fixed dipole of $\mu = 1$ D that is close to the calculated or observed value and sensitive to packing effects. We estimate the isotropic static polarizability of TTA to be 37 Å^3 based on toluene (12 Å^3) and aniline (12 Å^3). A correction-vector (CV) ZINDO calculation[34] returns principal values of 36.3, 72.6, and 72.6 Å^3 along the principal axes with Z along the three-fold axis; the CV-ZINDO isotropic value is roughly twice the value estimated from aniline and toluene polarizabilities The principal axes indicate an axial molecule. The ZINDO polarizabilities of TTA^+ and TTA^- are also axial. The isotropic average of TTA^+ increases to 85 Å^3, whereas the huge value of 250 Å^3 for TTA^- is expected but should not be taken too seriously. For randomly oriented TTA molecules, the dipole defines a local Z axis and the polarizability tensor $\alpha = (a, a, b)$ with an isotropic average of $(2a + b)/3$. We take $a = 2b = 44$ Å^3, which gives the experimental average and the calculated anisotropy.

The lattice model has electric field $\mathbf{A}_p$ at site p due to fixed dipoles and fields $\mathbf{E}_{qp}$ and $\mathbf{E}_{q'p}$ due to the cation at q and anion at q'. These fields generate induced dipoles $\mathbf{m}_p$ at all sites that contribute to the fields. Hence, self-consistent fields $\mathbf{F}_p$ due to dipoles and $\mathbf{F}_{qp}$ and $\mathbf{F}_{q'p}$ due to charges must be found. The procedure is well-known for organic molecular crystals.[11,32] The present simulations use a $(12)^3$ supercell as the repeat unit in a simple cubic lattice and an adaptive iterative method to achieve self-consistency. We construct the supercell to have no net dipole, i.e., $\Sigma_p \boldsymbol{\mu}_p = 0$, because the films are not ferroelectric. If it proves necessary, supercells that are an order of magnitude larger can be used. The following results are initial applications of self-consistent modeling of an amorphous film of polar and polarizable molecules.[35]

Point charges at adjacent sites separated by a distance d define a dipole ed whose electronic stabilization in the lattice is calculated to be 0.64 eV. The corresponding energy for forming ion pairs in polar solvents is small, ∼0.1 eV, and usually neglected.[3,4] Dipoles in solvents can reorient and shield Coulomb interactions as $1/\kappa R$ with the static dielectric constant $\kappa > 10$. In addition, there is a stabilization of ∼0.3 eV in polar films for placing (trapping) the electron at a site with high electrostatic potential and the hole on the neighbor with the lowest potential. The physical motivation is that electron mobility is low, if at all observable, and electrons are in deep (dipolar) traps.[6] Because holes are mobile, it is natural to form an ion pair at a trapped electron. A lattice based on molecular TTA properties stabilizes a TTA^+TTA^- pair by an additional 1.0 eV below the 4.28 eV for direct interactions. That is still ∼1 eV higher than the EL maximum at 2.13 eV. We cannot exclude EL from ions on adjacent TAPC molecules. Our reason for studying the intramolecular CT state was to minimize assumptions about the structure of the ion pair, which is not known in CL. Coupling through the sp^3 carbon favors intramolecular EL in TAPC films.

There are general reasons for expecting that lattice stabilization has been underestimated. We already noted[2] that charge localization in TTA^- increases E_{cd} by 0.1−0.2 eV on shifting the charge from a lattice point, for example, by localizing the negative charge on a phenyl ring. The electrostatic interactions being modeled are $1/r^4$ for charge−induced-dipole interaction and $1/r^5$ for dipole−induced-dipole interactions. A cubic lattice minimizes such contributions at fixed density. Indeed, a simple cubic lattice with $d = 8$ Å has a larger molecular volume than TTA and would require a smaller d value. Local variations in r are likely to increase the dipole stabilization by at least 20%, again by 0.1−0.2 eV, and we are trying to model such variations more quantitatively. Together, these changes increase the lattice contribution by ∼0.5 eV, but require additional model parameters.

In addition to lattice contributions, accurate structural information about ion pairs in films would also increase the direct interaction between TTA^+ and TTA^-. Our estimate of the charge−induced-dipole interaction has been piecemeal. The structural relaxation of the ions in Table 3 ignores relaxation about the sp^3 carbon of TAPC or molecular motions in films, the self-consistent electronic polarization of 0.93 eV is estimated above for an isolated ion pair, and the dipole stabilization of 0.64 eV is based on point charges and ignores the TTA^- dipole in Table 4.

An actual or hypothetical structure of the film is required for a joint modeling of charge redistribution around an ion pair. The TAPC molecule makes it possible to estimate the ion-pair energy as 3.3 eV with controlled approximations about its structure and about the polar medium. As noted above, lower ion-pair energy by an electronvolt can be rationalized by lattice and direct interactions that, however, require additional approximations about the local molecular environment. The present treatment supports the hypothesis that the EL maximum at 2.13 eV in TAPC films is emission from an ion pair.

V. Discussion and Summary

The strikingly different PL and EL of TAPC films, as well as the nature of the EL maximum at 580 nm,[1] motivated the present study. PL and EL spectra generally coincide in the organic solid state both for molecules and for conjugated polymers. Exceptional systems such as TAPC films must have special features that we summarize below. The previous section

enumerated the electrostatic stabilization of a TTA^+TTA^- ion pair in a polar lattice, with large contributions from the charge−induced-dipole interaction of the ions, from electronic polarization of the dipole, and from charge−dipole interactions that trap an anion with localized charge.

The absorption and PL spectra of TTA and TAPC are virtually identical in dilute dichloromethane solution.[1] The Stokes shift of 0.78 eV is due to molecular relaxation (0.26 eV) and interaction with the polar solvent. Large Stokes shifts in polar solvents are well-known for twisted intramolecular charge-transfer (TICT) complexes,[36] in which rotation about single bonds stabilizes the large dipole of the ion-pair excited state. TICTs show that single bonds provide sufficient coupling of π systems to sustain fluorescence. The intramolecular CT state of TAPC has poor π overlap and coupling through the sp^3 carbon; the state is reached by charge migration rather than by excited-state motion. The absorption spectra of TTA and TAPC films are again the same, but the PL spectra are not. The TAPC and TTA emission peaks at ~380 and 450 nm[1] are due to single molecules and aggregates, respectively. The latter is relatively much more intense in TTA, indicative of more extensive aggregation. Planar organic molecules are prone to aggregation in the excited state, as documented by excimer and exciplex emission. The TAPC structure (Figure 1) is less prone to aggregation for simple steric reasons.

The exciplex route for CL or electro-CL in solution requires ion pairs whose energy is below not only that of the lowest singlet, but also that of the lowest triplet of the donor and acceptor.[3–5] TTA was the donor of choice for CL, consistent with its triplet at almost 3 eV in Table 6. The TAPC triplet has equally high energy.[23] The exciplex route in solution invokes emission from a weakly bound ion pair that forms by anion and cation diffusion. Unless the energy is below E_T, triplet formation is possible and can be verified by fluorescence due to triplet−triplet annihilation. Exciplex emission demonstrates that anion−cation collisions lead to sufficient electronic overlap that is clearly required for direct recombination. In polar films with fixed dipoles, mobile electrons and holes in thermal equilibrium go to sites with the highest and lowest dipolar potential, respectively, according to E_{cd} in (eq 12). An ion pair in TAPC is mainly formed by hole mobility, which is well established for aromatic donors. The σ bridge in TAPC increases the overlap between TTA moieties beyond that of nonbonded neighbors. Such overlap facilitates ion-pair emission, for example, in TICTs,[36] but is not an absolute necessity. The dual emission reported by Rommens et al.[6] in thin-film devices based on TTA trimer also involves overlap, this time through a phenyl ring. We suppose that the EL peak around 575−595 nm[1] is an ion pair and the one around 450 nm is fluorescence of TTA aggregates. Dual emission can be rationalized by a distribution of site energies in polar films.

D'Andrade and Forrest[37] reported different PL and EL triplet emissions from films doped with a square-planar Pt complex, M = FPt1 = [2-(4′,6′-difluorophenyl)pyridinato-N,C^2]acetyl acetate. The PL peak at 610 nm is associated with a triplet excimer based on both experimental and theoretical characterization. The broad EL peak with a maximum at 690 nm is distinctly different and assigned to a triplet excimer, $^3D^*$, such as $(^3M^*)(^1M)$ where ^1M is the ground state. Their analysis, very similar to ours, is in terms of different photophysics for excitation with photons or e−h recombination.[37] Because EL is the basis for assigning $^3D^*$, the data allow the alternative interpretation of $^3(M^+M^-)$ and emission upon recombination of the ion pair. A low-energy CT state that is accessible in amorphous polar films upon charge injection, but not upon photoexcitation, is just as we propose for TAPC. Instead of an 80-nm red shift between EL and excimer PL in the triplet emission of the Pt complex, the singlet EL of TAPC is red-shifted by 130 nm from the PL maximum of aggregates. Detailed analysis of molecular excitations and their stabilization in polar films supports the formation of a low-energy ion pair in TAPC.

In this work, we obtained the electronic structure of TTA, its radical ions, TAPC, and TPD using ab initio methods for ground states and the PPP model for π-electron excitations. Calculated molecular properties such as electronic excitations, structures, and dipoles are in reasonable agreement with experiment. TAPC can accurately be viewed as a TTA dimer with uncoupled π systems but significant Coulomb interactions, whereas the π systems of TPD are coupled. Our calculations show conclusively that charge localization in TTA^- and the anion's polarizability strongly stabilize the intramolecular CT state of TAPC that corresponds to an ion pair, as shown in section III. The ion pair is further stabilized in a polar medium, as estimated in section IV, by charge−dipole interactions that act as charge traps and by electronic polarization. These results support the interpretation of direct emissive recombination of ions for the unusual EL of TAPC. Direct recombination is the exciplex route for CL in solution at far longer wavelength than molecular fluorescence. TAPC and a few other films are rare organic systems with strikingly different EL and PL spectra. PL involves excimer or aggregate emission, whereas EL at longer wavelength is plausibly assigned to direct recombination from an ion pair whose low energy was the focus of our study.

Acknowledgment. Z.G.S. thanks the Jawaharlal Nehru Centre for Advanced Scientific Research for a visiting professorship. The Department of Science and Technology partly supported this work through Project SR/S2/CMP-24/2003.

References and Notes

(1) Kalinowski, J.; Giro, G.; Cocchi, M.; Fattori, V.; Di Marco, P. *Appl. Phys. Lett.* **2000**, *76*, 2352.
(2) Soos, Z. G.; Mukhopadhyay, S.; Ramasesha, S. *Chem. Phys. Lett.* **2007**, *442*, 285.
(3) (a) Zachariasse, K. In *The Exciplex*; Gordon, M., Ware, W. R., Eds.; Academic Press, New York, 1975. p 273, (b) Weller, A. In *The Exciplex*; Gordon, M., Ware, W. R., Eds.; Academic Press, New York, 1975; p 23.
(4) Keszthelyi, C. P.; Bard, A. J. *Chem. Phys. Lett.* **1974**, *24*, 300. Park, S. M.; Bard, A. J. *J. Am. Chem. Soc.* **1975**, *97*, 2978.
(5) Armstrong, N. R.; Wightman, R. M.; Gross, E. *Annu. Rev. Phys. Chem.* **2001**, *52*, 391.
(6) Rommens, J.; Vaes, A.; Van der Auweraer, M.; De Schryver, F. C.; Bassler, H.; Pommerehne, J. *J. Appl. Phys.* **1998**, *84*, 4487.
(7) Van der Auweraer, M.; De Schryver, F. C.; Borsenberger, P. M.; Bässler, H. *Adv. Mater.* **1994**, *6*, 199.
(8) Bässler, H. *Phys. Status Solidi* **1993**, *B175*, 15.
(9) Borsenberger, P. M.; Weiss, D. S. *Organic Photoreceptors for Imaging Systems*; Marcel Dekker: New York, 1993, and references therein.
(10) Anusooya, Y.; Pati, S. K.; Ramasesha, S. *J. Chem. Phys.* **1997**, *106*, 10230.
(11) Silinsh, E. A.; Cápek, V. *Organic Molecular Crystals*; AIP Press: New York, 1994, and references therein.
(12) Reynolds, S. L.; Scaringe, R. P. *Cryst. Struct. Commun.* **1982**, *11*, 1129. Sobolev, A. N.; Belsky, V. K.; Romm, I. P.; Yu, N.; Guryanova, E. N. *Acta Crystallogr.* **1985**, *C41*, 967.
(13) Hill, I. G.; Kahn, A.; Soos, Z. G.; Pascal, R. A. *Chem. Phys. Lett.* **2000**, *327*, 181.
(14) Sakanoue, K.; Motoda, M.; Sugimoto, M.; Sakaki, S. *J. Phys. Chem. A* **1999**, *103*, 5551.
(15) Young, R. H.; Fitzgerald, J. J. *J. Phys. Chem.* **1995**, *99*, 4230.
(16) Manifar, T.; Robani, S.; Jennings, M.; Hairsine, D.; Dance, I. *Cryst. Eng. Commun.* **2006**, *8*, 59.
(17) Pople, J. A. *Trans. Faraday Soc.* **1953**, *49*, 1375. Pariser, R.; Parr, R. G. *J. Chem. Phys.* **1953**, *21*, 767.

(18) Ohno, K. *Theor. Chim. Acta* **1964**, *2*, 219.
(19) Szabo, A.; Ostlund, N. S. *Modern Quantum Chemistry: Introduction to Advanced Electronic Structure Theory*; MacMillan: New York, 1982.
(20) Streitwieser, A., Jr. *Molecular Orbital Theory for Organic Chemists*; Wiley: New York, 1961. Parr, R. G. *The Quantum Theory of Molecular Electronic Structure*; W. A. Benjamin: New York, 1963.
(21) Slater, J. C.; Koster, G. F. *Phys. Rev.* **1954**, *94*, 1498.
(22) Liang, C. J.; Zhao, D.; Hong, Z. R.; Li, R. G.; Yu, J. Q. *Thin Solid Films* **2000**, *371*, 207.
(23) Hensel, K.; Bässler, H. *Adv. Mater. Opt. Electron.* **1992**, *1*, 179.
(24) Tsuboi, T.; Murayama, H.; Penzkofer, A. *Thin Solid Films* **2006**, *499*, 306.
(25) Zerner, M. C.; Loew, G. H.; Kirchner, R. F.; Mueller-Westerhoff, U. T. *J. Am. Chem. Soc.* **1980**, *102*, 589.
(26) Granick, S.; Michaelis, L. *J. Am. Chem. Soc.* **1940**, *62*, 2241.
(27) Rittner, E. S. *J. Chem. Phys.* **1951**, *19*, 1030.
(28) Soos, Z. G.; Hayden, G. W.; McWilliams, P. C. M.; Etemad, E. *J. Chem. Phys.* **1990**, *93*, 7439. Soos, Z. G.; Hennessy, M. H.; Wen, G. *Chem. Phys.* **1998**, *227*, 19.
(29) Pati, S. K. Ph.D. Thesis, Indian Institute of Sciences, Bangalore, India, 1998.
(30) Paolini, J. P. *J. Comput. Chem.* **1990**, *11*, 1160.
(31) Albert, I. D. L., Ph.D. Thesis, Indian Institute of Sciences, Bangalore, India, 1991.
(32) Tsiper, E. V.; Soos, Z. G. *Phys. Rev. B* **2001**, *64*, 195124; *Phys. Rev. B* **2003**, *68*, 085301.
(33) Sin, J. M.; Soos, Z. G. *Philos. Mag.* **2003**, *83*, 901.
(34) Ramasesha, S.; Shuai, Z.; Bredas, J. L. *Chem. Phys. Lett.* **1996**, *245*, 224.
(35) Topham, B. J.; Soos, Z. G. Princeton University, Princeton, NJ. Unpublished results, 2007.
(36) Sun, X.; Liu, Y.; Xu, X.; Yu, G.; Chen, S.; Qiu, W.; Ma, Y.; Zhao, Z.; Zhu, D. *Synth. Met.* **2006**, *156*, 1174. (a) Ghoneim, N.; Suppan, P. *Pure Appl. Chem.* **1993**, *65*, 1739.
(37) D'Andrade, B.; Forrest, S. R. *Chem. Phys.* **2003**, *286*, 321.

JP8012078